HHS Public Access

Author manuscript

Neurochem Int. Author manuscript; available in PMC 2020 July 01.

Published in final edited form as:

Neurochem Int. 2019 July ; 127: 137–147. doi:10.1016/j.neuint.2018.12.016.

Developmental differences in microglia morphology and gene expression during normal brain development and in response to hypoxia-ischemia

Pelin Cengiz[*,1,2], **Dila Zafer**[2], **Jayadevi H Chandrashekhar**[2,3], **Vishal Chanana**[2], **Jacob Bogost**[2], **Alex Waldman**[2,4], **Becca Novak**[2], **Douglas B Kintner**[2], **Peter A Ferrazzano**[1,2]

[1]Department of Pediatrics, University of Wisconsin School of Medicine and Public Health, Madison, WI, USA

[2]Waisman Center, University of Wisconsin School of Medicine and Public Health, Madison, WI, USA

[3]University of Illinois at Urbana-Champaign, IL, USA

[4]Emory University School of Medicine, Atlanta, GA, USA

Abstract

Background: Neuroinflammation plays an important role in ischemic brain injury and recovery, however the interplay between brain development and the neuroinflammatory response is poorly understood. We previously described age-dependent differences in the microglial response and the effect of microglial inhibition. Here we investigate whether age-dependent microglial responses may be related to pre-injury developmental differences in microglial phenotype.

Methods: Measures of microglia morphology were quantified using semi-automated software analysis of immunostained sections from postnatal day 2 (P2), P9, P30 and P60 mice using IMARIS. Microglia were isolated from P2, P9, P30 and P60 mice, and expression of markers of classical and alternative microglial activation was assessed, as well as transforming growth factor beta (TGF-β) receptor, Serpine1, Mer Tyrosine Kinase (MerTK), and the suppressor of cytokine signaling (SOCS3). Hypoxia-ischemia (HI) was induced in P9 and P30 mice using unilateral carotid artery ligation and exposure to 10% oxygen for 50 minutes. Microglia morphology and microglial expression of genes in the TGF-β and MerTK pathways were determined in ipsilateral and contralateral hippocampus.

Results: A progressive and significant increase in microglia branching morphology was seen in all brain regions from P2 to P30. No consistent classical or alternative activation profile was seen in isolated microglia. A clear transition to increased expression of TGF-β and its downstream

[*]Corresponding author address: Pelin Cengiz, MD, University of Wisconsin-Madison, Department of Pediatrics, 1500 Highland Ave - T505, Madison, WI 53705-9345, United States, Phone: (608) 263-8552, cengiz@wisc.edu.

Conflict of interest:
Author state no conflict of interest.

effector serpine1 was seen between P9 and P30. A similar increase in expression was seen in MerTK and its downstream effector SOCS3. HI resulted in a significant decrease in branching morphology only in the P9 mice, and expression of TGF-β receptor, Serpine1, MerTK, and SOCS3 were elevated in P30 mice compared to P9 post-HI.

Conclusion: Microglia maturation is associated with changes in morphology and gene expression, and microglial responses to ischemia in the developing brain differ based on the age at which injury occurs.

Keywords

microglia; hypoxia-ischemia; brain development; pediatrics

1. Introduction:

Microglia are the primary immune response cells in the brain, and play an important role both in maintaining homeostasis during normal brain function and in directing the inflammatory response to infection or injury. Derived from myeloid precursor cells originating in the yolk sac, microgliapopulate the brain in the early embryonic period (Ginhoux et al., 2010). During fetal brain development, microgliademonstrate an ameboid morphology consistent with motility and the phagocytosis of debris resulting from apoptosis and synaptic pruning (Czeh et al., 2011; Paolicelli et al., 2011). Perinatally, microglia with an ameboid morphology migrate throughout the brain along developing white matter tracts, and spread into gray matter where they transition into a highly ramified, immunosurveillance morphology which is maintained throughout life (Hristova et al., 2010; Rezaie, 2003). The time-course of this transition from ameboid to ramified morphology in microglial phenotype in the developing brain is yet to be characterized to a full extent.

Neuroinflammation is a key player in the brain's response to ischemic insult, with both a pro-inflammatory cytotoxic component (Biran et al., 2006; Deng, 2010; Yenari et al., 2006), and an anti-inflammatory neurotrophic component (Butovsky et al., 2006; Lalancette-Hebert et al., 2007; Walton et al., 2006). Consequently, modulating the microglial response to injury has been proposed as a potential therapeutic target after brain injury. We previously described age-dependent differences in the microglial response to hypoxic-ischemic (HI) injury in the developing brain, with important implications for therapies targeting post-injury neuroinflammation (Cikla et al., 2016a; Ferrazzano et al., 2013). We found that microglia in newborn postnatal day 9 (P9) mice respond to hypoxia-ischemia (HI) with increased activation, proliferation and release of pro-inflammatory cytokines compared to juvenile P30 mice (Ferrazzano et al., 2013). We subsequently found differential effects of suppressing the microglial response after HI between P9 and P30 mice (Cikla et al., 2016a). Minocycline effectively suppressed the early microglial response to HI in both age groups of mice, however only the P30 mice demonstrated sustained improvements in brain atrophy and neurologic function. Thus, we hypothesized that the developmental differences in microglial response to HI may be related to baseline differences in microglial phenotype due to the ongoing microglial maturation process during brain development. Therefore in this study, in order to determine if microglial ramification differs between ages, we first quantitatively defined the evolution of microglia morphology from the neonatal to the adult period.

Microglial activation is associated with a transformation from a ramified morphology with a small cell body and highly branched filamentous cell processes, to one with a large cell body and short, stout, unbranched cell processes, similar to that observed early in brain development (Harry, 2013). Microglia exhibit two general categories of activation, one characterized by secretion of pro-inflammatory and cytotoxic cytokines (M1, classical activation), and another defined by expression of immunomodulatory and neurotrophic factors (M2, alternative activation) (Cherry et al., 2014; David and Kroner, 2011; Martinez et al., 2009). In order to determine whether developmental changes in microglia morphology are associated with differences in microglial activation state, we characterized the developmental profile of microglial markers of classical and alternative microglia activation pathways.

Recent research has focused on characterizing microglia-specific gene expressions in order to identify microglia subtypes and potential targets for modulating microglia function (Butovsky et al., 2014; Das et al., 2015; Doorn et al., 2015; Erny et al., 2015; Hickman et al., 2013; Parakalan et al., 2012). The Transforming Growth Factor-beta (TGF-β) receptor and Mer Tyrosine Kinase (MerTK), have been identified as components of a unique molecular signature in adult microglia (Butovsky et al., 2014). Both of these signaling pathways have important roles in microglial function during normal brain development and in response to an insult, making them potential mediators of age-related differences in microglial responses to injury. TGF-β is necessary for microglial maturation, induces microglial quiescence, and directs microglia towards M2 activation in response to an insult (Abutbul et al., 2012; Butovsky et al., 2014; Zhou et al., 2012). MerTK mediates microglial phagocytosis of apoptotic cells in neurogenic brain regions, and suppresses inflammation through expression of the suppressor of cytokine signaling (SOCS1 and SOCS3) (Fourgeaud et al., 2016; Rothlin et al., 2007). To explore whether age-dependent differences in the microglial response to injury may be related to developmental differences in microglial TGF-β and MerTK signaling, we defined the developmental profile of TGF-β and MerTK pathway expressions in the developing brain under physiological conditions and following HI.

Here we present the age-dependent differences in microglia morphology and gene expression in the downstream signaling of the TGF-β and MerTK pathways in response to HI.

2. Methods:

2.1. Animal use:

All procedures used mice with C57BL/6J background and were carried out in adherence with the NIH Guide for the Care and Use of Laboratory Animals using protocols reviewed by the Institutional Animal Care and Use Committee at our institution. All efforts were made to minimize animal suffering, to reduce the number of animals used, and to utilize alternatives to in vivo techniques, if available. Male and female mice in each age group were included in each experiment in order to address the sex as a variable.

2.2. Induction of neonatal HI:

HI was induced as previously described with some modifications (Vannucci and Vannucci, 1997). Postnatal day (P) 9 C57BL/6J mice were anesthetized with isofluorane (5% for induction, 2-3% for maintenance; Butler Schein Animal Health Supply) in 1 lt/min nitrous oxide and 0.3 lt/min oxygen. The body temperature of the pups was maintained at 36 °C using a heated surgical table (Molecular Imaging Products). Under a surgical microscope (Nikon SMZ-800 Zoom Stereo, Nikon), a midline skin incision was made and the muscle overlying the trachea visualized. The left common carotid artery was freed from the carotid sheath by blunt dissection, electrically cauterized, and cut. The incision was injected with 0.5% bupivacaine and closed with a single 6.0 silk suture. Animals were returned to their dams and monitored continuously for a 2 hour (h) recovery period. To induce unilateral ischemic injury, following the recovery period the animals were placed in a hypoxia chamber (BioSpherix) equilibrated with 10% O_2 and 90% N_2 at 36-37°C for 50 min. After HI, animals were returned to their dams and monitored for pain and discomfort every minute (min) for the first 30 min, every 30 min for the next 2 h, and then daily until sacrificed at 2 days post-injury. This is a wellcharacterized model of neonatal HI and results in reproducible brain injury ipsilateral (IL) to the electrocauterized left common carotid artery (Vannucci and Vannucci, 1997) (Cengiz et al., 2011; Uluc et al., 2013) (Cikla et al., 2016b) (Cikla et al., 2016a). In this model, unilateral severing of common carotid artery alone does not induce ischemic injury due to collateral circulation from the contralateral (CL) side through the circle of Willis. Only subsequent exposure of mice to hypoxic air mixture results in hemispheric ischemia as a result of the preferential decrease of blood flow to the ipsilateral (IL) hemisphere secondary to hypocarbia (Mujsce et al., 1990). Sham-operated mice received anesthesia and exposure of the left common carotid artery without electrocauterization or hypoxia, as described in this model before (Cikla et al., 2016a; Cikla et al., 2016b; Fang et al., 2013).

2.3. Immunohistochemistry:

Mice were deeply anesthetized with 5% isoflurane and transcardially perfused with 4% paraformaldehyde (PFA) (pH 7.4). After post-fixation of the brains in 4% PFA overnight, brains were subsequently cryoprotected in a 30% sucrose/PBS solution for 48 h. Frozen brains were cut into coronal sections (35 μm) on a freezing microtome (Leica SM 2000R; Buffalo Grove, IL), and stored in antifreeze solution at -20°C. For immunofluorescence staining, free floating mid-hippocampus sections were washed three times with 0.1M Tris-buffered saline (TBS) and then subjected to 10 mM Sodium Citrate solution (pH 8.5) for 30 minutes at 80 °C for antigen retrieval. Subsequently, slices were blocked with TBS^{++} (0.1% Triton X-100 and 3% goat serum in 0.1 M TBS) for 60 min at room temperature. Slices were double-stained with anti-Iba1 (1:250 diluted in TBS^{++}; rabbit polyclonal, WAKO, Richmond, VA) and anti-MAP2 (1:500 diluted in TBS^{++}; mouse monoclonal, Sigma, St. Louis, MO) for 1 h at 37°C and then overnight at 4°C with mild shaking. After washing with TBS (3 x 10 min), brain sections were incubated with the appropriate secondary antibodies (goat antirabbit Alexa Fluor 488-conjugated IgG (1:200 diluted in TBS^{++}) and goat anti-mouse Alexa Fluor 546-conjugated IgG (1:200 diluted in TBS^{++}) for 1 h at 37°C. Slices were washed with TBS (3 x 10 min) slices and mounted on slides using Vectashield mounting media with DAPI (Vector Labs, Burlingame, CA). For every stained slide there

was corresponding negative antibody control staining in which primary antibodies were eliminated to serve as negative control for nonspecific secondary antibody staining. Slides were imaged with a Nikon A1R-Si confocal microscope using a 20X or 60X objective.

2.4. Microscopy and Morphometric analysis:

Z-stack (1 μm intervals) images (512 x 512 pixels) of brain sections were acquired using a 60X oil objective on a Nikon A1R-Si confocal microscope. Semi-automated image analysis was performed using Bitplane IMARIS 8.0. 3D image analysis software (Oxford Instruments, Concord, MA) based on a previously described method (Nayak et al., 2013). Morphometric analysis was performed on Iba1 positive microglia in images acquired from cortex, CA1 hippocampus, and striatum. Images were subjected to maximum intensity projection (MIP) and only microglia whose processes were entirely within the 3-D Z-stack volume were quantified. Five to ten microglia were analyzed per brain region assessed in each mouse (n=6-8 mice/group). Microglia ramification was quantified on MIP images using automatic filament tracing to determine total process length, number of branch points, number of end-points, and number of branch segments (Morrison and Filosa, 2013). Manual filament tracing was performed instead of automated method in P9 post-HI samples due to the dramatic alteration in microglia morphology in these specimens. Soma volume was determined from surface render images, and the process end-points were used to create a hull volume representing the 3-D volume of tissue surveilled by each microglia.

2.5. Microglia isolation and Quantitative Polymerase chain Reaction (qRT-PCR):

Mice were perfused with once with PBS (pH 7.4) transcardially. Then brains are removed from the skull, and brain tissues were processed using a Neural tissue dissociation kit (Miltenyi Biotec, San Diego, CA). Whole brain samples or pooled samples from 5 mice for the regions of cortex, striatum and hippocampus are used to isolate microglia by magnetic-activated cell sorting using CD1 lb-conjugated magnetic bead separation (Miltenyi Biotec, San Diego, CA). RNA was extracted from microglia using Qiagen RNeasy mini-spin kit (Qiagen Inc, Valencia, CA). RNA concentration and purity were determined using a NanoDrop 2000c (Thermo Scientific, Waltham MA), and cDNA was synthesized from 250 ng total RNA using a SuperScript® VILO™ cDNA kit (Invitrogen, Waltham, MA). Taqman Low-Density Array Cards (Applied Biosystems, Foster City, CA) were used to assess developmental profiling of the gene expressions of tumor necrosis factor-alpha (TNF-alpha), interleukin 1 beta (IL-1β), inducible nitric oxide synthase (iNOS), CD32, CD206, TGF-β receptor 1 (TGFβR1), Serpine1, MerTK and SOCS3 in microglia isolated from whole brain samples of P2, P9, P30 and P60 mice. Beta-actin and ribosomal 18s were used as reference genes. For post-HI assessment of TGF-β and MerTK pathway genes, TaqMan Gene Expression Assay probes were used for TGF-β, TGF-β1 receptor, Serpine1, Growth arrest specific protein (Gas6), MerTK, SOCS3, and beta actin (reference gene) in microglia isolated from ipsilateral and contralateral hippocampi of P9 and P30 mice. A master mix solution was made consisting of 0.5 μl TaqMan gene expression assay probe (20X), 7.5 μl TaqMan Gene expression master mix, and 5.0 μl nuclease free water and samples loaded on a 384 well plate with a final reaction volume of 15 μl. qPCR was performed using the ViiA-7 Real Time PCR System (Applied Biosystems) following the manufacturer's instructions. All samples were run in duplicates, relative gene expression was calculated

using the ΔΔCt method normalized to a single biological sample used on all plates, and expression is presented as fold change versus the control group as indicated in figure legends (Fig. 4 and 6).

2.6. Statistical Analysis:

Statistical tests were performed using SPSS Statistics version 24.0 (IBM Corporation). For developmental profile of morphologic measures, three-way MANOVA was performed to test for main effects and interaction effects between age, sex and brain region, with Bonferroni alpha correction of between-subjects effects for the multiple morphologic measurements, followed by Tamhane's post-test in the morphologic measures that demonstrated significant between-subjects effects and at least a 2-fold change in expression. For developmental gene expression analysis, two-way MANOVA was used to test for main effects and interaction effects between age and sex, with Bonferroni corrected p-value for between-subjects effects in multiple genes assessed, followed by Tukeys post hoc test for group comparisons in genes with significant between-subjects effects. For post-HI morphometrics, paired t-test was used to test for within brain differences in morphologic measures between ipsilateral and contralateral hemispheres. For gene expression analysis post-HI, three-way MANOVA was used to test for main effects and interaction effects between age, sex and HI, with between-subjects p-value Bonferroni-corrected for multiple genes assessed, followed by Tukeys post-test in genes with significant between-subject effects and at least a 2-fold change in expression. Results were considered to be statistically significant if p-value<0.05.

Results:

3.1. Developmental profile of microglia morphology.

We first set out to characterize developmental changes in microglia distribution and morphology. Immunostaining for microglia and neurons was performed in P2, P9, P30 and P60 mice. As shown in Figure 1, microglia in the neonatal P2 brain demonstrate a scattered distribution and an ameboid morphology with few cell processes. In P9 brains, microglia are more diffuse throughout grey matter regions, with an increase in cell processes. In P30 and P60 brains, microglia are evenly distributed throughout the brain, and demonstrate a highly ramified morphology with abundant branched and filamentous cell processes.

Next, we quantified these morphologic changes using semi-automated software analysis of microglia branching and cell body size. As shown in the representative images of hippocampal microglia from P2-P60 brains in Figure 2, consecutive Z-stack images were used to create a maximum intensity projection (MIP; a,f,k,p)and 3-dimensional surface render (b,g,l,q) of individual microglia. Skeletonized images (c,h,m,r) were used to calculate measures of microglia branch length and number of branch segments, junctions and end-points for each microglia. A hull surface render (d,i,n,s) was created for each microglia using the branch endpoints, representing the volume of tissue surveilled by each individual microglia. Microglia soma volumes (e,j,o,t) were calculated from surface render images. The progressive increase in microglia ramification seen qualitatively in these images is quantified in Figure 3. Overall, a progressive increase in measures of microglia branching and decrease in cell body size is seen from P2 to P30 in each brain region. Microglia total branch length

(A), branch points (B) number of segments (C), and terminal points (D) were significantly greater in P30 brain regions compared to P2 and P9 brain regions (3-4 fold increase vs P2, ~2 fold increase vs P9, $p<0.05$). Hull volume (E) of P30 mice was 10-fold larger than P2 mice and 3-fold greater than P9. In contrast, soma volume (F) demonstrated approximately a 40% reduction in volume between P2 and P30 mice. No difference in morphology measures was found between P30 and P60 mice, and no significant differences were seen between brain regions or males and females. In summary, microglia undergo significant changes in morphology during normal brain development, and reach a mature phenotype by P30.

3.2. Profile of microglia gene expression in the developing brain

We next set out to determine whether microglia gene expression profile is associated with developmental changes in microglia morphology. The immature microglia phenotype, consisting of ameboid microglia and microglia with few stout cell processes, is similar to the morphology seen in activated microglia responding to neurologic insult (Hanisch and Kettenmann, 2007) (Harry and Kraft, 2012). Therefore, expression of genes associated with classical activation (M1), and alternative activation (M2) were assessed in microglia isolated from whole brain specimens of P2, P9, P30 and P60 mice. Additionally, we assessed expression of genes in the TGF-β and MerTK pathways, known to be important in directing microglia development and activation responses (Butovsky et al., 2014). As shown in Figure 4, while a number of M1 and M2 genes demonstrated significant differences between age groups, no clear M1 or M2 profile is seen in microglia isolated from the developing brain. Among the antiinflammatory M2 genes (Fig. 4 E-H), Arg1 demonstrated a dramatic reduction in expression in the P30 and P60 microglia compared to P2 and P9, while the expression of YM1 was significantly increased in the older age groups, and IL-10 was increased only in P60 mice. Expression of pro-inflammatory genes was more consistent across age groups (Fig. 4 A-D). There was a significant increase only in IL-1β expression and iNOS expression microglia from P60 and P9 mice, respectively, with no difference seen in TNF-alpha and CD32 expressions.

In contrast to the M1 and M2 genes, expression of genes in the TGF-β and MerTK pathways demonstrated a clear developmental transition between P9 and P30 (Fig. 4 I-L). Expression of TGFβR1 was 5 fold greater in P30 and P60 mice compared to P2 and P9. Expression of the downstream effector of TGF-β receptor signaling, Serpine1, was also dramatically increased in the older age groups ($p<0.05$). Expression of MerTK and the downstream effector, suppressor of cytokine signaling 3 (SOCS3) were significantly increased in P30 and P60 mice compared to P2 and P9 mice.

3.3. Effect of HI on microglia in the developing brain

Having identified significant differences in microglia morphology and expression of genes in the TGF-β and MerTK signaling pathways between P9 and P30 mice, we next set out to determine whether exposure to HI affects microglia morphology and TGF-β/MerTK signaling differently between P9 and P30 mice. Two days after induction of HI, microglia morphology was quantified from immunostaining of the ipsilateral (hypoxic-ischemic hemisphere) and contralateral (hypoxia-only, in-situ control) hippocampus. Representative images of microglia morphology in ipsilateral and contralateral P9 and P30 hippocampus are

shown in Figure 5 A-B. Microglia in contralateral hippocampus of P9 and P30 mice retain a branched morphology. In ipsilateral hippocampus of P9 mice, microglia are seen to have few cell processes with little branching. In contrast, microglia in ipsilateral P30 hippocampus retain a highly ramified morphology. As shown in Figure 5 C-H, HI resulted in a significant reduction in microglia branching measures and hull volume in ipsilateral hippocampus of only P9 mice. A consistent but not significant decrease in morphological measures was seen in ipsilateral P30 microglia.

We next assessed the effect of HI on expression of genes in the TGF-β and MerTK pathways in microglia isolated from P9 and P30 hippocampus at 2 days post-HI. As shown in Figure 6, HI did not significantly affect expression of TGF-β (A) or the ligand for MerTK, Gas6 (D). However, HI resulted in a significant reduction in expression of the TGF-β receptor in ipsilateral hippocampus in both P9 and P30 mice (B). Interestingly, HI resulted in a significant increase in expression of Serpine1 in CD11b+ microglia/macrophages isolated from ipsilateral hippocampus of P9 mice, while no change was seen in P30 mice (C). However, expression of TGF-βR1 and Serpine1 remained significantly elevated in P30 ipsilateral microglia/macrophages compared to ipsilateral P9. HI resulted in a significant decrease in expression of MerTK and SOCS3 in ipsilateral P9 and P30 hippocampal microglia/macrophages (E and F). Again, expression of both the receptor and downstream effector remained significantly elevated in the ipsilateral P30 compared to ipsilateral P9 hippocampus.

4. Discussion:

4.1. Microglia in the developing brain.

Microglia originate from yolk sac-derived myeloid precursor cells and colonize the brain during early embryonic period (Czeh et al., 2011; Ginhoux et al., 2010). In the early fetal brain, microglia are ameboid phagocytic cells thought to be responsible for clearance of cellular debris occurring from normal brain development (Graeber and Streit, 2010; Paolicelli et al., 2011). During the late fetal period, microglia migrate along developing white matter tracts and spread into gray matter regions (Rezaie, 2003). In early postnatal brain development, microglia begin a morphologic transition from ameboid cell into the highly ramified morphology found in the adult brain (Hristova et al., 2010).

In our prior studies, we found developmental differences in microglial responses to injury between infant and juvenile mice (Cikla et al., 2016a; Ferrazzano et al., 2013), and questioned whether differential microglia responses may be related to phenotypic differences between neonatal and juvenile microglia. Therefore, in the current study, we quantitatively describe microglia morphology at time-points during the first two months of brain development. We found a progressive increase in microglia branching measures from P2 to P30 and a concomitant decrease in cell body size. Microglia in the P2 brain exhibited large cell bodies with few short unbranched cell processes. By P9, microglia total cell process length and number of branch points had approximately doubled, with another doubling of these measures occurring between P9 and P30. In contrast, no change in microglia morphometrics was found between P30 and P60, indicating that microglia in the juvenile brain have attained a mature phenotype.

Microglial morphology is closely related to microglia function. Highly ramified microglia found in the mature brain are associated with an immunosurveillance state, and maintenance of homeostasis in the neuronal and synaptic environment (Hanisch and Kettenmann, 2007; Harry, 2013). In response to an injury or pathogen exposure, microglial activation involves a transition from a highly ramified morphology to one with increased cell body size and short stout cell processes. In some cases, microglial activation can progress to a complete ameboid phagocytic morphology. The immature microglial morphology we observed at P2 and P9 is consistent with an “activated” phenotype, reflecting a role in phagocytosis and synaptic pruning during the early postnatal period. Given this activated morphology in immature microglia, we assessed for age differences in the expression of genes associated with classical (M1) and alternative (M2) activation states found in microglial and macrophage responses to injury and infection. Expression of M1 and M2 markers has been observed in neonatal microglia (Lenz et al., 2013), but the developmental profile of this expression has not been previously described to our knowledge. Classical activation is associated with pro-inflammatory cytokine expression, such as TNF-alpha, IL-1beta, iNOS, and CD32 (David and Kroner, 2011). Not surprisingly, microglia isolated from naïve brains demonstrated overall low levels of these pro-inflammatory markers in each age group, with the exception of an increase in IL-1beta in P60 mice and iNOS in P9 mice. Alternative activation is associated with expression of immunomodulatory and anti-inflammatory cytokines such as Arg1 , IL-10, YM1 and CD206, and promotes phagocytosis and wound healing (Cherry et al., 2014). Among M2 genes, we found a dramatic increase in Arg1 expression in P2 and P9 mice compared to P30 and P60. Interestingly, the reverse expression pattern was seen in expression of YM1, with an increase in expression in the older age groups. Arg1 converts L-arginine to prolines and polyamines, competes with iNOS for substrate, and has been described to have a role in tissue remodeling and repair (Munder, 2009) (Corraliza et al., 1995). YM1 is a secretory lectin which binds heparin and prevents breakdown of the extra cellular matrix (Chang et al., 2001) (Hung et al., 2002). This transition in M2 profile from predominantly Arg1 in the immature brain to YM1 expression in the mature brain may therefore be associated with a transition in the role of microglia from supporting the remodeling of the developing brain to supporting homeostasis in the mature brain. Regardless, it will be important to consider these developmental differences in M1 and M2 gene expression when markers of classical and alternative activation are assessed in future developmental brain injury studies.

It is important to note that while describing microglia polarization in terms of M1/M2 activation states is a useful framework for understanding pro- vs. anti-inflammatory microglial responses, it clearly oversimplifies the heterogeneity of the microglial population, particularly within the alternative activation profile where a number of subtypes of microglia function have been described. The M2a response is mediated through IL4 and functions to suppress inflammation (Pepe et al., 2014), whereas the toll-like receptor-mediated M2b response is suggested to have a role in initiating microglia immunoregulatory M2 responses (Chhor et al., 2013), and signaling through IL10 and TGF-beta yields the M2c profile, thought to be primarily associated with tissue remodeling (Cherry et al., 2014). Even this subclassification likely obscures the complexity of microglial responses, which is perhaps

more appropriately viewed as a spectrum of integrated individual microglia profiles, each with specific roles in in the overall inflammatory response.

TGFβR1 and MerTK were recently identified as part of a unique molecular signature in adult microglia when compared to neonatal microglia, cultured microglia, and microglial cell line culture (Butovsky et al., 2014). Additionally, TGF-β and TAM kinase signaling pathways are important mediators of microglia function in both the normal brain and in response to injury (Massague, 2012; Rothlin et al., 2015). Therefore, we examined the expression of these receptors and their downstream signaling proteins in the developing brain. Interestingly, we found a transition in expression of the TGF-β receptor and MerTK receptor between P9 and P30 which mirrors the transition in microglia morphology that occurs at this time. A similar increase was seen in the expression of Serpine1 and SOCS3, indicating increased activity of T TGFβR1 and MerTK signaling in the juvenile and adult microglia compared to infant and neonatal microglia.

TGF-β is a pleiotrophic growth factor which plays an essential role in developmental programs regulating cell proliferation, differentiation and regeneration (Massague, 2012). Activation of the TGFβR1 by binding of TGF-β results in upregulation of SMAD-mediated gene expression, including Serpine1. TGF-β receptor signaling through SMAD3 pathways has been suggested to be responsible for inducing a quiescent microglial phenotype (Abutbul et al., 2012), and TGF-β expression is necessary for normal microglial development (Butovsky et al., 2014). Knockout of TGF-β results in a severe inflammatory condition and death by 3 weeks of age, and accordingly, TGF-β deficiency has been proposed to contribute to autoimmune pathologies (Bommireddy et al., 2003). In our study, increase in TGFβR1 expression and downstream signaling was associated with a developmental transition in microglia phenotype to a highly ramified immunosurveillance cell, consistent with the role of TGF-β signaling in maintaining microglial quiescence in the mature brain.

MerTK is a member of the tyr/axl/mer (TAM) family of kinases, responsible for inhibiting inflammation via expression of the suppressor of cytokine signaling proteins, SOCS1 and SOCS3 (Rothlin et al., 2007). TAM kinases are therefore responsible for suppressing inflammation in the absence of an inflammatory stimulus, and in restoring normal immune function after an injury or infection. Knockout of TAM kinases induces an increase in basal activation of pro-inflammatory signaling through MAP kinases and NF-kB (Ji et al., 2013), and results in chronic inflammation and systemic autoimmunity (Lu and Lemke, 2001). Additionally, TAM kinases play a role in mediating microglial phagocytosis. MerTK and its ligand Gas6 regulate clearance of the apoptotic cells associated with adult neurogenesis, and knockout of MerTK results in accumulation of apoptotic debris in neurogenic regions (Fourgeaud et al., 2016). Apoptotic cell death is a normal and essential component of early brain development (Mazarakis et al., 1997; Yamaguchi and Miura, 2015) (Roth and D'Sa, 2001), and clearance of this debris is commonly cited as an important role for microglia in the developing brain (Bilimoria and Stevens, 2015; Casano and Peri, 2015; Harry, 2013). However, we found that MerTK expression and downstream signaling is increased in microglia present in older compared to younger mice, suggesting that the role of MerTK in microglial phagocytosis may be specific to mature microglia. Regardless, the increase in MerTK expression between P9 and P30 is consistent with the transition to a mature

morphology, and the role of ramified microglia in maintaining immune homeostasis in the healthy adult brain.

4.2. Age differences in gene expression in microglia/macrophages in response to HI

Consistent with our previous findings (Ferrazzano et al., 2013) (Cikla et al., 2016a), in the current study we found that HI results in intense microglia activation in ipsilateral hippocampus of P9 mice, with microglia demonstrating a significant decrease in branching measures and an increase in cell body volume. In contrast, HI induced a much more moderate decrease in branching morphology in the P30 microglia, which overall retained a highly ramified morphology. We previously found that these phenotypic differences in microglia morphology were associated with a more pro-inflammatory cytokine expression profile in P9 mice compared to P30 mice (Ferrazzano et al., 2013). In interpreting these results, it is important to consider the contribution of developmental and regional differences in susceptibility to HI-induced neuronal and oligodendrocyte cell death. For example, developmental differences in sub-cortical white matter injury have been described in the hypoxia-ischemia model (Albertsson et al., 2014), as well as the selective vulnerability of the hippocampus to hypoxic-ischemic injury (Schmidt-Kastner, 2015; Schmidt-Kastner and Freund, 1991; Semple et al., 2013; Towfighi et al., 1997). We focused the current investigation on HI-induced microglia activation in the hippocampus because we have found this to be the most consistently injured brain region post-HI (Cikla et al., 2016a; Cikla et al., 2016b; Uluc et al., 2013), and we previously demonstrated that HI induces a similar degree of early hippocampal injury between P9 and P30 mice (Ferrazzano et al., 2013). Whether the developmental differences seen in the microglia response following HI is due to primary effect of HI or secondary to age-and region-dependent differences in neuronal or glial susceptibility to HI, needs to be studied further.

To explore mechanisms which may underlie developmental differences in the microglial response to HI, we first identified a clear developmental transition in microglial TGF-β and MerTK signaling pathways during normal brain development, and then assessed for differences in the effect of HI on these pathways between P9 and P30 mice. Our interest in these pathways stems from their importance both in establishing and maintaining the immunosurveillance mode of microglia, and also in directing microglial responses to injury. We found that HI affected microglial gene expression in the TGF-β and MerTK pathways differently between age groups. In the TGF-β pathway, HI resulted in an increase in SMAD-mediated downstream signaling in the P9 mice, as evidenced by a significant increase in Serpine1 expression. While Serpine1 expression was not changed in P30 mice, its expression remained dramatically elevated compared to P9. TGF-β exposure has been shown to direct microglia towards M2 responses (Zhou et al., 2012), induce microglial expression of anti-inflammatory genes (Paglinawan et al., 2003), and inhibit secretion of pro-inflammatory factors (Liu et al., 2016). Increased signaling through the TGF-β pathway in P30 mice compared to P9 mice after HI, is therefore consistent with our previous findings of a more balanced pro- vs. ant-inflammatory cytokine profile in P30 mice after HI (Ferrazzano et al., 2013).

When we examined the effect of HI on the MerTK pathway, we found a reduction in MerTK expression and downstream signaling in both age groups in response to HI, however P30 microglia again demonstrated significantly increased expression compared to P9. MerTK signaling plays an important role in downregulating the immune response after an injury, and knockout of the ligand or receptor results in prolonged microglial activation and pro-inflammatory cytokine release (Ji et al., 2013) (Gruber et al., 2014). Additionally, TAM kinases have been implicated in promoting remyelination after white matter injury. Myelin removal is a critical first step in the remyelinating process (Kotter et al., 2005), and efficient phagocytosis of myelin debris is necessary for remyelination to occur (Lampron et al., 2015). As mentioned previously, Gas6-MerTK signaling plays a key role in directing microglial phagocytosis, and Gas6 knockout mice demonstrate delayed remyelination and impaired maturation of preoligodendrocytes after experimental demyelination (Binder et al., 2011) (Gruber et al., 2014). Interestingly, a recent study has linked TGF-β and MerTK in microglial phagocytosis of myelin. Healy et al found that exposure of human microglia to TGF-β resulted in upregulation of MerTK expression and enhanced ingestion of myelin by microglia, and that this TGF-β-mediated phagocytosis could be blocked by inhibition of MerTK (Healy et al., 2016). We previously described sustained white matter injury in P9 mice after HI (Uluc et al., 2013), and our current study demonstrates decreased MerTK signaling in P9 mice in response to HI, suggesting that TGF-β and MerTK pathways may be potential therapeutic targets for neonatal HI-induced white matter injury. Further study will be needed to define the role of the TGF-β and MerTK pathways in the microglial response to HI in the developing brain.

4.3. Sex differences in microglia morphology and gene expressions following HI:

In our studies, we did not see any sex differences in the microglial morphological transition from immature to mature phenotype, or in the expressions of the TGF-β and TAM kinase signaling pathways during development and following HI. Sex differences in the number of microglia and microglial morphology has been described previously in the neonatal hypothalamus at P0-P2 (Schwarz et al., 2012) (Lenz and McCarthy, 2015) and hippocampus at P4, and a role in regulating synaptic patterning selectivity in developing brains has been established. These studies suggest that sex differences in microglia morphology and function are highly region and age specific, and further study is warranted to determine whether sex-differences exist in microglia TGF-β and TAM kinase signaling in specific regions and timepoints after HI.

5. Conclusion

In summary, microglia demonstrate a transition from immature to mature morphology between P9 and P30, and this phenotypic change is associated with an increase in expression in the TGF-β and TAM kinase signaling pathways seen in P30 and P60 mice. Hypoxic-ischemic insult induces differential changes in morphology and in TGF-β and MerTK signaling, and the effect of modulating the microglial response to HI via manipulation of these pathways warrants further study. Age-dependent differences in the microglial response to injury will need to be carefully considered as therapies targeting microglia are developed for pediatric brain injury.

Acknowledgements:

We thank Dr. Knobel, Dr. Svaren, J. Pinnow, D. Bollig, and R. Emerson at the Waisman Center IDDRC Model Core. This work was supported by NIH/NINDS K08NS078113 (P. Ferrazzano), NIH/NINDS K08NS088563-01 (P Cengiz), Department of Pediatrics Research & Development Grant (P. Ferrazzano and P Cengiz) and NIH grant P30 HD03352 (Waisman Center).

References

Abutbul S, Shapiro J, Szaingurten-Solodkin I, Levy N, Carmy Y, Baron R, Jung S, Monsonego A, 2012 TGF-beta signaling through SMAD2/3 induces the quiescent microglial phenotype within the CNS environment. Glia 60, 1160–1171. [PubMed: 22511296]

Albertsson AM, Bi D, Duan L, Zhang X, Leavenworth JW, Qiao L, Zhu C, Cardell S, Cantor H, Hagberg H, Mallard C, Wang X, 2014 The immune response after hypoxiaischemia in a mouse model of preterm brain injury. J Neuroinflammation 11, 153. [PubMed: 25187205]

Bilimoria PM, Stevens B, 2015 Microglia function during brain development: New insights from animal models. Brain Res 1617, 7–17. [PubMed: 25463024]

Binder MD, Xiao J, Kemper D, Ma GZ, Murray SS, Kilpatrick TJ, 2011 Gas6 increases myelination by oligodendrocytes and its deficiency delays recovery following cuprizone-induced demyelination. PLoS One 6, e17727. [PubMed: 21423702]

Biran V, Joly LM, Heron A, Vernet A, Vega C, Mariani J, Renolleau S, Charriaut-Marlangue C, 2006 Glial activation in white matter following ischemia in the neonatal P7 rat brain. Exp Neurol 199, 103–112. [PubMed: 16697370]

Bommireddy R, Ormsby I, Yin M, Boivin GP, Babcock GF, Doetschman T, 2003 TGF beta 1 inhibits Ca2+-calcineurin-mediated activation in thymocytes. J Immunol 170, 3645–3652. [PubMed: 12646629]

Butovsky O, Jedrychowski MP, Moore CS, Cialic R, Lanser AJ, Gabriely G, Koeglsperger T, Dake B, Wu PM, Doykan CE, Fanek Z, Liu L, Chen Z, Rothstein JD, Ransohoff RM, Gygi SP, Antel JP, Weiner HL, 2014 Identification of a unique TGF-beta-dependent molecular and functional signature in microglia. Nat Neurosci 17, 131–143. [PubMed: 24316888]

Butovsky O, Ziv Y, Schwartz A, Landa G, Talpalar AE, Pluchino S, Martino G, Schwartz M, 2006 Microglia activated by IL-4 or IFN-gamma differentially induce neurogenesis and oligodendrogenesis from adult stem/progenitor cells. Mol Cell Neurosci 31, 149–160. [PubMed: 16297637]

Casano AM, Peri F, 2015 Microglia: multitasking specialists of the brain. Dev Cell 32, 469477.

Cengiz P, Kleman N, Uluc K, Kendigelen P, Hagemann T, Akture E, Messing A, Ferrazzano P, Sun D, 2011 Inhibition of Na+/H+ exchanger isoform 1 is neuroprotective in neonatal hypoxic ischemic brain injury. Antioxid Redox Signal. 14, 1803–1813. doi: 1810.1089/ars.2010.3468. Epub 2010 Dec 1804. [PubMed: 20712402]

Chang NC, Hung SI, Hwa KY, Kato I, Chen JE, Liu CH, Chang AC, 2001 A macrophage protein, Ym1, transiently expressed during inflammation is a novel mammalian lectin. J Biol Chem 276, 17497–17506. [PubMed: 11297523]

Cherry JD, Olschowka JA, O'Banion MK, 2014 Neuroinflammation and M2 microglia: the good, the bad, and the inflamed. J Neuroinflammation 11, 98. [PubMed: 24889886]

Chhor V, Le Charpentier T, Lebon S, Ore MV, Celador IL, Josserand J, Degos V, Jacotot E, Hagberg H, Savman K, Mallard C, Gressens P, Fleiss B, 2013 Characterization of phenotype markers and neuronotoxic potential of polarised primary microglia in vitro. Brain Behav Immun 32, 70–85. [PubMed: 23454862]

Cikla U, Chanana V, Kintner DB, Covert L, Dewall T, Waldman A, Rowley P, Cengiz P, Ferrazzano P, 2016a Suppression of microglia activation after hypoxia-ischemia results in age-dependent improvements in neurologic injury. Journal of neuroimmunology 291, 18–27. [PubMed: 26857490]

Cikla U, Chanana V, Kintner DB, Udho E, Eickhoff J, Sun W, Marquez S, Covert L, Otles A, Shapiro RA, Ferrazzano P, Vemuganti R, Levine JE, Cengiz P, 2016b ERalpha Signaling Is Required for

TrkB-Mediated Hippocampal Neuroprotection in Female Neonatal Mice after Hypoxic Ischemic Encephalopathy(1,2,3). eNeuro 3.

Corraliza IM, Soler G, Eichmann K, Modolell M, 1995 Arginase induction by suppressors of nitric oxide synthesis (IL-4, IL-10 and PGE2) in murine bone-marrow-derived macrophages. Biochem Biophys Res Commun 206, 667–673. [PubMed: 7530004]

Czeh M, Gressens P, Kaindl AM, 2011 The yin and yang of microglia. Dev Neurosci 33, 199–209. [PubMed: 21757877]

Das A, Chai JC, Kim SH, Park KS, Lee YS, Jung KH, Chai YG, 2015 Dual RNA sequencing reveals the expression of unique transcriptomic signatures in lipopolysaccharideinduced BV-2 microglial cells. PLoS One 10, e0121117. [PubMed: 25811458]

David S, Kroner A, 2011 Repertoire of microglial and macrophage responses after spinal cord injury. Nat Rev Neurosci 12, 388–399. [PubMed: 21673720]

Deng W, 2010 Neurobiology of injury to the developing brain. Nat Rev Neurol 6, 328–336. [PubMed: 20479779]

Doorn KJ, Breve JJ, Drukarch B, Boddeke HW, Huitinga I, Lucassen PJ, van Dam AM, 2015 Brain region-specific gene expression profiles in freshly isolated rat microglia. Front Cell Neurosci 9, 84. [PubMed: 25814934]

Erny D, Hrabe de Angelis AL, Jaitin D, Wieghofer P, Staszewski O, David E, Keren-Shaul H, Mahlakoiv T, Jakobshagen K, Buch T, Schwierzeck V, Utermohlen O, Chun E, Garrett WS, McCoy KD, Diefenbach A, Staeheli P, Stecher B, Amit I, Prinz M, 2015 Host microbiota constantly control maturation and function of microglia in the CNS. Nat Neurosci 18, 965–977. [PubMed: 26030851]

Fang AY, Gonzalez FF, Sheldon RA, Ferriero DM, 2013 Effects of combination therapy using hypothermia and erythropoietin in a rat model of neonatal hypoxia-ischemia. Pediatr Res 73, 12–17. [PubMed: 23085817]

Ferrazzano P, Chanana V, Kutluay U, Fidan E, Akture E, Kintner DB, Cengiz P, Sun D, 2013 Age-dependent microglial activation in immature brains after hypoxia-ischemia. CNS NEUROL DISORD-DR 12, 338–349.

Fourgeaud L, Traves PG, Tufail Y, Leal-Bailey H, Lew ED, Burrola PG, Callaway P, Zagorska A, Rothlin CV, Nimmerjahn A, Lemke G, 2016 TAM receptors regulate multiple features of microglial physiology. Nature 532, 240–244. [PubMed: 27049947]

Ginhoux F, Greter M, Leboeuf M, Nandi S, See P, Gokhan S, Mehler MF, Conway SJ, Ng LG, Stanley ER, Samokhvalov IM, Merad M, 2010 Fate mapping analysis reveals that adult microglia derive from primitive macrophages. Science 330, 841–845. [PubMed: 20966214]

Graeber MB, Streit WJ, 2010 Microglia: biology and pathology. Acta Neuropathol 119, 89–105. [PubMed: 20012873]

Gruber RC, Ray AK, Johndrow CT, Guzik H, Burek D, de Frutos PG, Shafit-Zagardo B 2014 Targeted GAS6 delivery to the CNS protects axons from damage during experimental autoimmune encephalomyelitis. J Neurosci 34, 16320–16335. [PubMed: 25471571]

Hanisch UK, Kettenmann H, 2007 Microglia: active sensor and versatile effector cells in the normal and pathologic brain. Nat Neurosci 10, 1387–1394. [PubMed: 17965659]

Harry GJ, 2013 Microglia during development and aging. Pharmacol Ther 139, 313–326. [PubMed: 23644076]

Harry GJ, Kraft AD, 2012 Microglia in the developing brain: a potential target with lifetime effects. Neurotoxicology 33, 191–206. [PubMed: 22322212]

Healy LM, Perron G, Won SY, Michell-Robinson MA, Rezk A, Ludwin SK, Moore CS, Hall JA, Bar-Or A, Antel JP, 2016 MerTK Is a Functional Regulator of Myelin Phagocytosis by Human Myeloid Cells. J Immunol 196, 3375–3384. [PubMed: 26962228]

Hickman SE, Kingery ND, Ohsumi TK, Borowsky ML, Wang LC, Means TK, El Khoury J, 2013 The microglial sensome revealed by direct RNA sequencing. Nat Neurosci. 16, 1896–1905. [PubMed: 24162652]

Hristova M, Cuthill D, Zbarsky V, Acosta-Saltos A, Wallace A, Blight K, Buckley SM, Peebles D, Heuer H, Waddington SN, Raivich G, 2010 Activation and deactivation of periventricular white matter phagocytes during postnatal mouse development. Glia 58, 11–28. [PubMed: 19544386]

Hung SI, Chang AC, Kato I, Chang NC, 2002 Transient expression of Ym1, a heparin binding lectin, during developmental hematopoiesis and inflammation. J Leukoc Biol 72, 72–82. [PubMed: 12101265]

Ji R, Tian S, Lu HJ, Lu Q, Zheng Y, Wang X, Ding J, Li Q, Lu Q, 2013 TAM receptors affect adult brain neurogenesis by negative regulation of microglial cell activation. J Immunol 191, 6165–6177. [PubMed: 24244024]

Kotter MR, Zhao C, van Rooijen N, Franklin RJ, 2005 Macrophage-depletion induced impairment of experimental CNS remyelination is associated with a reduced oligodendrocyte progenitor cell response and altered growth factor expression. Neurobiol Dis 18, 166–175. [PubMed: 15649707]

Lalancette-Hebert M, Gowing G, Simard A, Weng YC, Kriz J, 2007 Selective ablation of proliferating microglial cells exacerbates ischemic injury in the brain. J Neurosci 27, 2596–2605. [PubMed: 17344397]

Lampron A, Larochelle A, Laflamme N, Prefontaine P, Plante MM, Sanchez MG, Yong VW, Stys PK, Tremblay ME, Rivest S, 2015 Inefficient clearance of myelin debris by microglia impairs remyelinating processes. J Exp Med 212, 481–495. [PubMed: 25779633]

Lenz KM, McCarthy MM, 2015 A starring role for microglia in brain sex differences. Neuroscientist 21, 306–321. [PubMed: 24871624]

Lenz KM, Nugent BM, Haliyur R, McCarthy MM, 2013 Microglia are essential to masculinization of brain and behavior. J Neurosci 33, 2761–2772. [PubMed: 23407936]

Liu Z, Chen HQ, Huang Y, Qiu YH, Peng YP, 2016 Transforming growth factor-beta1 acts via TbetaR-I on microglia to protect against MPP(+)-induced dopaminergic neuronal loss. Brain Behav Immun 51, 131–143. [PubMed: 26254549]

Lu Q, Lemke G, 2001 Homeostatic regulation of the immune system by receptor tyrosine kinases of the Tyro 3 family. Science 293, 306–311. [PubMed: 11452127]

Martinez FO, Helming L, Gordon S, 2009 Alternative activation of macrophages: an immunologic functional perspective. Annu Rev Immunol 27, 451–483. [PubMed: 19105661]

Massague J, 2012 TGFbeta signalling in context. Nat Rev Mol Cell Biol 13, 616–630. [PubMed: 22992590]

Mazarakis ND, Edwards AD, Mehmet H, 1997 Apoptosis in neural development and disease. Arch Dis Child Fetal Neonatal Ed 77, F165–170. [PubMed: 9462183]

Morrison HW, Filosa JA, 2013 A quantitative spatiotemporal analysis of microglia morphology during ischemic stroke and reperfusion. J Neuroinflammation 10, 4. [PubMed: 23311642]

Mujsce DJ, Christensen MA, Vannucci RC, 1990 Cerebral blood flow and edema in perinatal hypoxic-ischemic brain damage. Pediatr Res 27, 450–453. [PubMed: 2345670]

Munder M, 2009 Arginase: an emerging key player in the mammalian immune system. Br J Pharmacol 158, 638–651. [PubMed: 19764983]

Nayak D, Johnson KR, Heydari S, Roth TL, Zinselmeyer BH, McGavern DB, 2013 Type I interferon programs innate myeloid dynamics and gene expression in the virally infected nervous system. PLoS Pathog 9, e1003395. [PubMed: 23737750]

Paglinawan R, Malipiero U, Schlapbach R, Frei K, Reith W, Fontana A, 2003 TGFbeta directs gene expression of activated microglia to an anti-inflammatory phenotype strongly focusing on chemokine genes and cell migratory genes. Glia 44, 219–231. [PubMed: 14603463]

Paolicelli RC, Bolasco G, Pagani F, Maggi L, Scianni M, Panzanelli P, Giustetto M, Ferreira TA, Guiducci E, Dumas L, Ragozzino D, Gross CT, 2011 Synaptic pruning by microglia is necessary for normal brain development. Science 333, 1456–1458. [PubMed: 21778362]

Parakalan R, Jiang B, Nimmi B, Janani M, Jayapal M, Lu J, Tay SS, Ling EA, Dheen ST, 2012 Transcriptome analysis of amoeboid and ramified microglia isolated from the corpus callosum of rat brain. BMC Neurosci 13, 64. [PubMed: 22697290]

Pepe G, Calderazzi G, De Maglie M, Villa AM, Vegeto E, 2014 Heterogeneous induction of microglia M2a phenotype by central administration of interleukin-4. J Neuroinflammation 11, 211. [PubMed: 25551794]

Rezaie P, 2003 Microglia in the Human Nervous System. Neuroembryology and Aging 2, 14.

Roth KA, D'Sa C, 2001 Apoptosis and brain development. Mental retardation and developmental disabilities research reviews 7, 261–266. [PubMed: 11754520]

Rothlin CV, Carrera-Silva EA, Bosurgi L, Ghosh S, 2015 TAM receptor signaling in immune homeostasis. Annu Rev Immunol 33, 355–391. [PubMed: 25594431]

Rothlin CV, Ghosh S, Zuniga EI, Oldstone MB, Lemke G, 2007 TAM receptors are pleiotropic inhibitors of the innate immune response. Cell 131, 1124–1136. [PubMed: 18083102]

Schmidt-Kastner R, 2015 Genomic approach to selective vulnerability of the hippocampus in brain ischemia-hypoxia. Neuroscience 309, 259–279. [PubMed: 26383255]

Schmidt-Kastner R, Freund TF, 1991 Selective vulnerability of the hippocampus in brain ischemia. Neuroscience. 40, 599–636. [PubMed: 1676492]

Schwarz JM, Sholar PW, Bilbo SD, 2012 Sex differences in microglial colonization of the developing rat brain. J Neurochem 120, 948–963. [PubMed: 22182318]

Semple BD, Blomgren K, Gimlin K, Ferriero DM, Noble-Haeusslein LJ, 2013 Brain development in rodents and humans: Identifying benchmarks of maturation and vulnerability to injury across species. Prog Neurobiol 106–107, 1–16.

Towfighi J, Mauger D, Vannucci RC, Vannucci SJ, 1997 Influence of age on the cerebral lesions in an immature rat model of cerebral hypoxia-ischemia: a light microscopic study. Brain Res Dev Brain Res 100, 149–160. [PubMed: 9205806]

Uluc K, Kendigelen P, Fidan E, Zhang L, Chanana V, Kintner D, Akture E, Song C, Ye K, Sun D, Ferrazzano P, Cengiz P, 2013 TrkB receptor agonist 7, 8 dihydroxyflavone triggers profound gender- dependent neuroprotection in mice after perinatal hypoxia and ischemia. CNS Neurol Disord Drug Targets 12, 360–370. [PubMed: 23469848]

Vannucci RC, Vannucci SJ, 1997 A model of perinatal hypoxic-ischemic brain damage. Ann N Y Acad Sci 835, 234–249. [PubMed: 9616778]

Walton NM, Sutter BM, Laywell ED, Levkoff LH, Kearns SM, Marshall GP 2nd, Scheffler B, Steindler DA, 2006 Microglia instruct subventricular zone neurogenesis. Glia 54, 815–825. [PubMed: 16977605]

Yamaguchi Y, Miura M, 2015 Programmed cell death in neurodevelopment. Dev Cell 32, 478–490. [PubMed: 25710534]

Yenari MA, Xu L, Tang XN, Qiao Y, Giffard RG, 2006 Microglia potentiate damage to blood-brain barrier constituents: improvement by minocycline in vivo and in vitro. Stroke 37, 1087–1093. [PubMed: 16497985]

Zhou X, Spittau B, Krieglstein K, 2012 TGFbeta signalling plays an important role in IL4-induced alternative activation of microglia. J Neuroinflammation 9, 210. [PubMed: 22947253]

Highlights:

- Microglia undergo significant changes in morphology during normal brain development, reaching a mature phenotype by P30.
- Microglia demonstrate a clear transition in expression of genes in the TGFb and MerTK signaling pathways between P9 and P30.
- Hypoxia-ischemia induces differential changes in microglia morphology as well as TGFb and MerTK signaling between P9 and P30 mice.

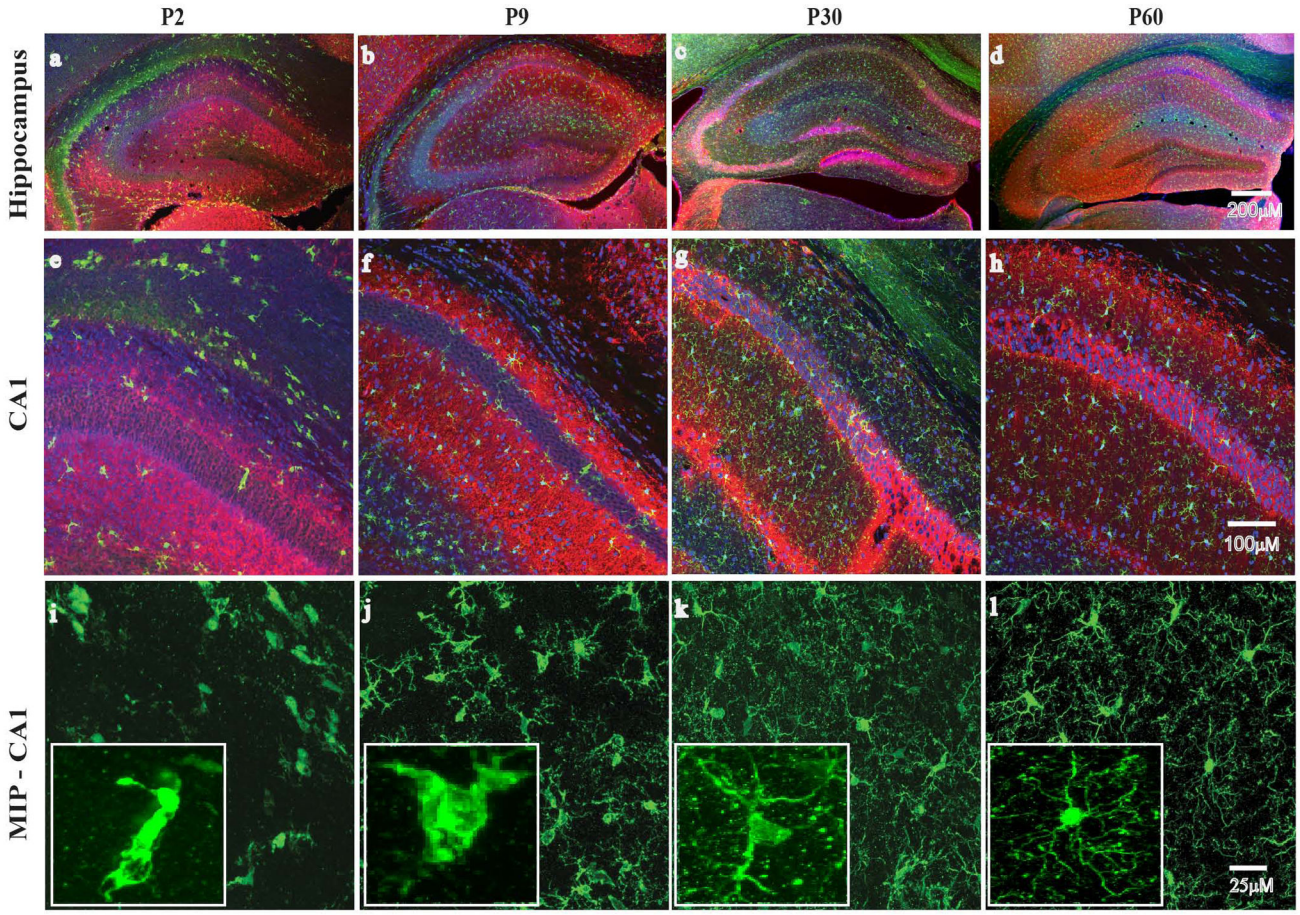

Figure 1: Age dependent differences in microglia morphology in the hippocampus.

Immunohistological staining for microglia (Iba1, green) and neurons (MAP2, red) in the hippocampus is shown (4X). Nuclei were stained with DAPI (blue). Regional distribution and morphology of microglia evolves with age in postnatal day 2 (P2), day 9 (P9), juvenile (P30) and adult (P60) mice. Microglia in the immature brain are concentrated in white matter regions bordering the hippocampus (a-d). With increasing age, microglia become more evenly distributed throughout the CA1 (20X) region (e-g), and demonstrate an increasingly ramified morphology (i-l and insets) (60X).

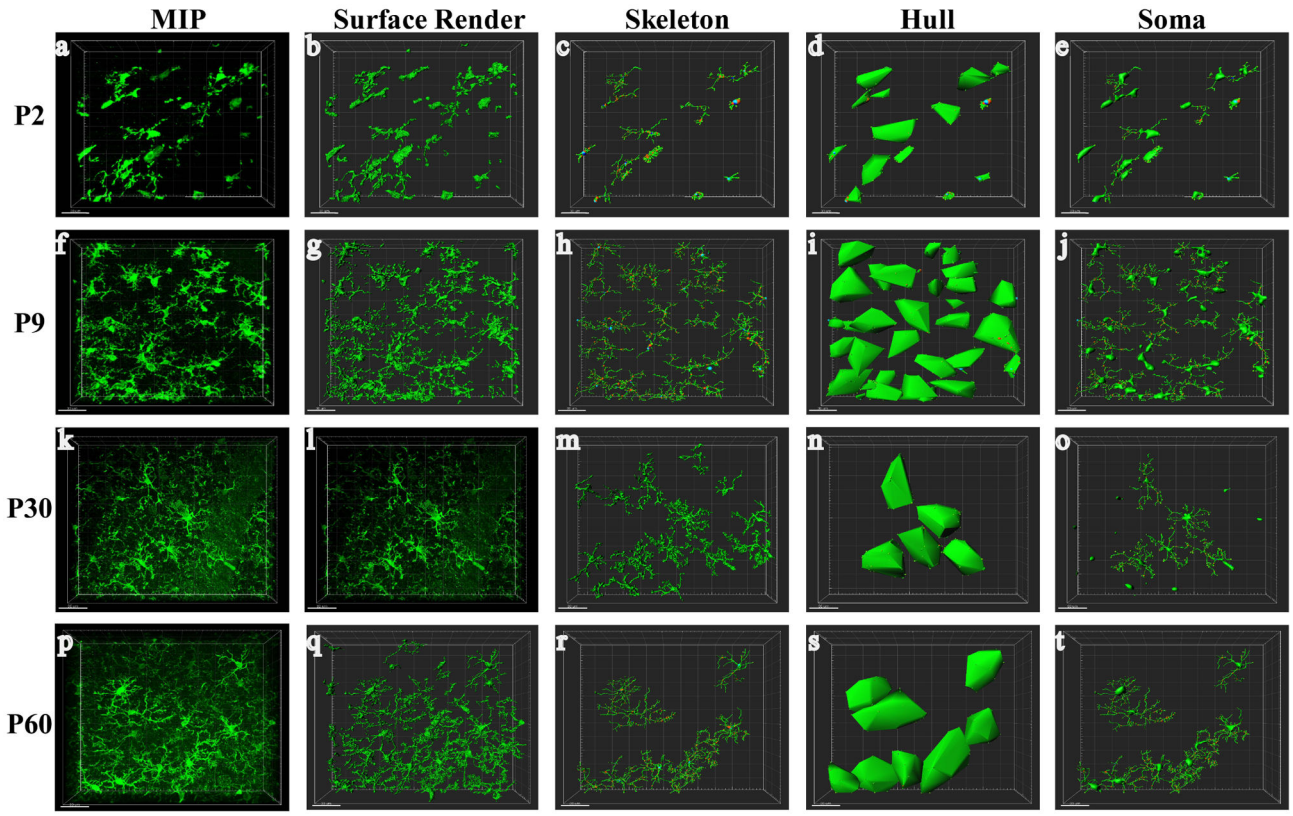

Figure 2: Morphometric analysis of microglia.

Z-stack confocal images were acquired at 1-μm intervals. Representative images from the CA1 region of P2, P9, P30 and P60 mice are shown demonstrating the IMARIS workflow. Consecutive Z-stack images were converted to a maximum intensity projection (MIP; a, f, k, p) and surface render (b, g, l, q). Images were skeletonized for quantification of branching measures (c, h, m, r). A hull surface render was created for each microglia using the cell process end-points (d, I, n, s). Soma were identified on surface renders for calculation of soma volume (e, j, o, t).

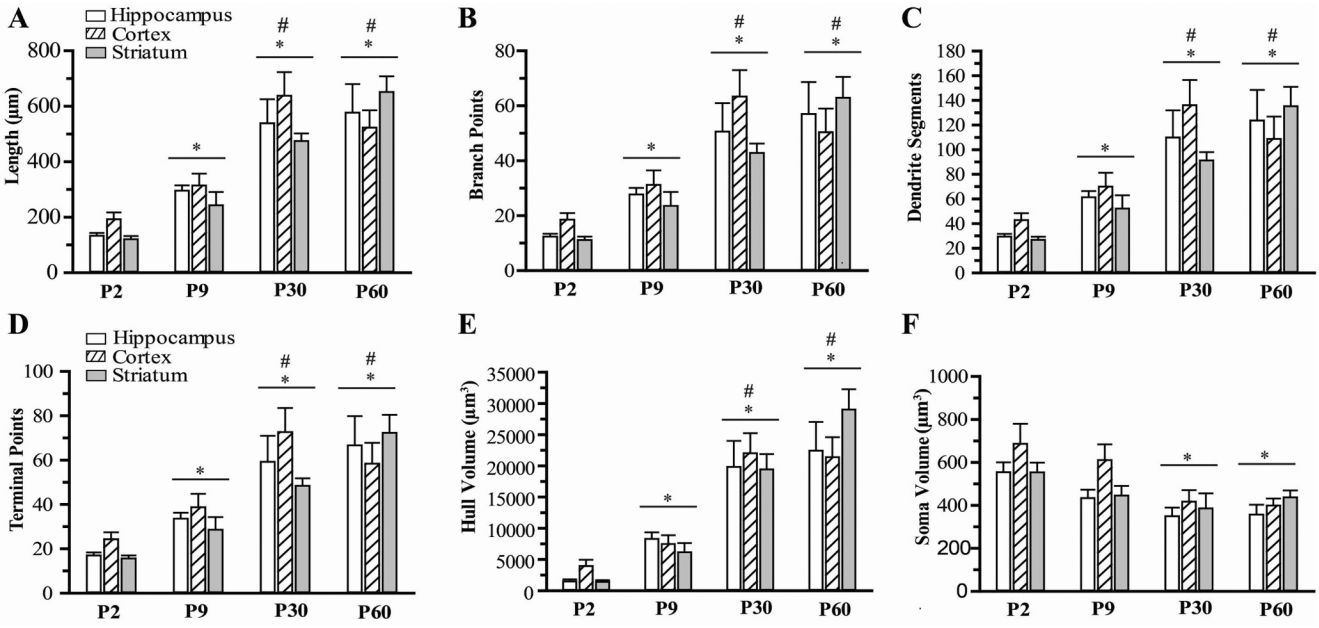

Figure 3: Quantification of microglial morphology.

The total branch length (A) and the number of number of branch points (B), branch segments (C), and terminal end points (D) were calculated from skeletonized images in CA1 hippocampus, cortex and striatum. The Hull volume and soma volume are shown in E and F, respectively. N=8-12 microglia/region/mouse, 6-9 mice/group. Mean ± SEM. * $p<0.05$ vs. P2 group, #$p<0.05$ vs P9 group.

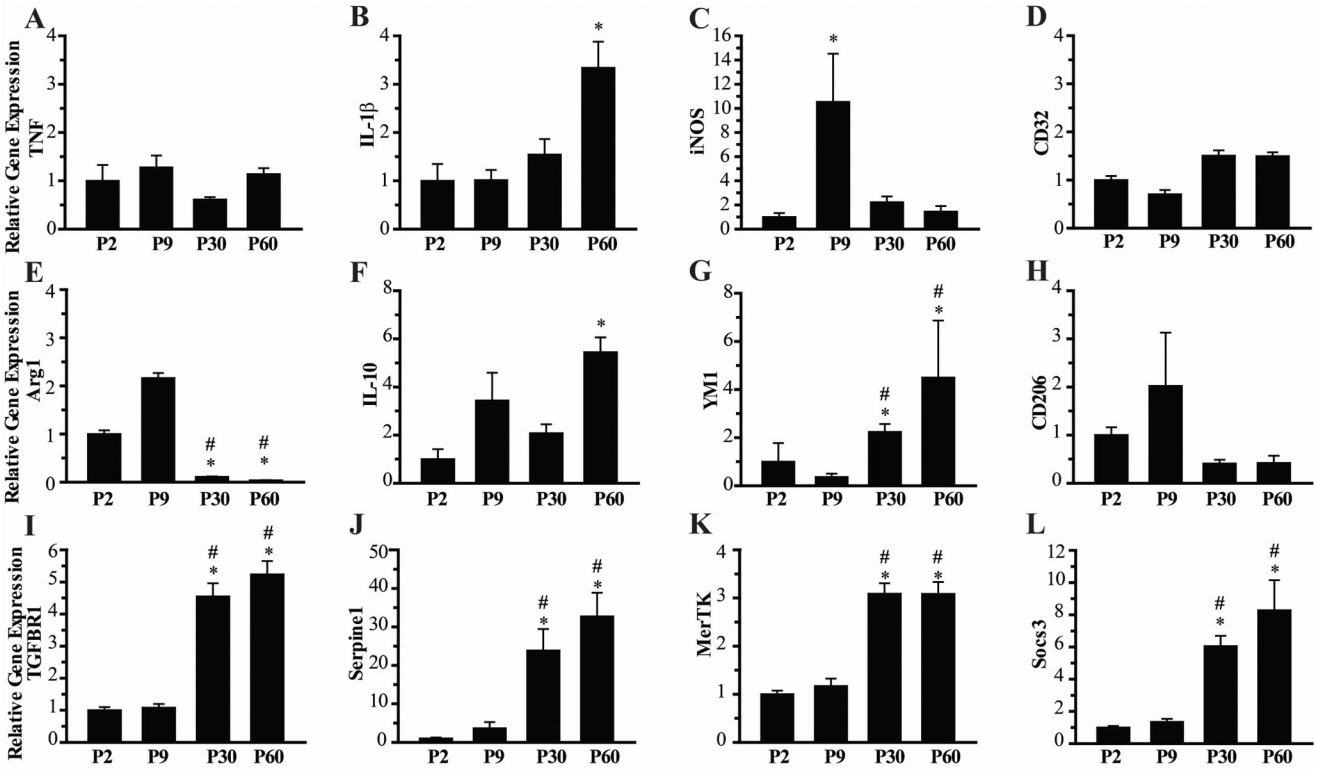

Figure 4: Age-dependent microglial gene expression.

Analysis of a panel of microglia genes is shown for microglia isolated from whole brains of P2, P9, P30 and P60 mice. Expression of markers of classical microglial activation (M1) are shown in A-D, and markers of alternative (M2) microglial activation are shown in E-H. Expression of the receptor for transforming growth factor beta (TGF-βR) and its downstream effector serpine1 are shown in I and J, respectively. Expression of Mer-Tyrosine Kinase (MERTK) and its downstream effector the suppressor of cytokine signaling (SOCS3) are shown in K and L. Expression is shown as fold change compared to P2 group, N=8 mice/group, Mean ± SEM. *p<0.05 vs P2, #p<0.05 vs P9.

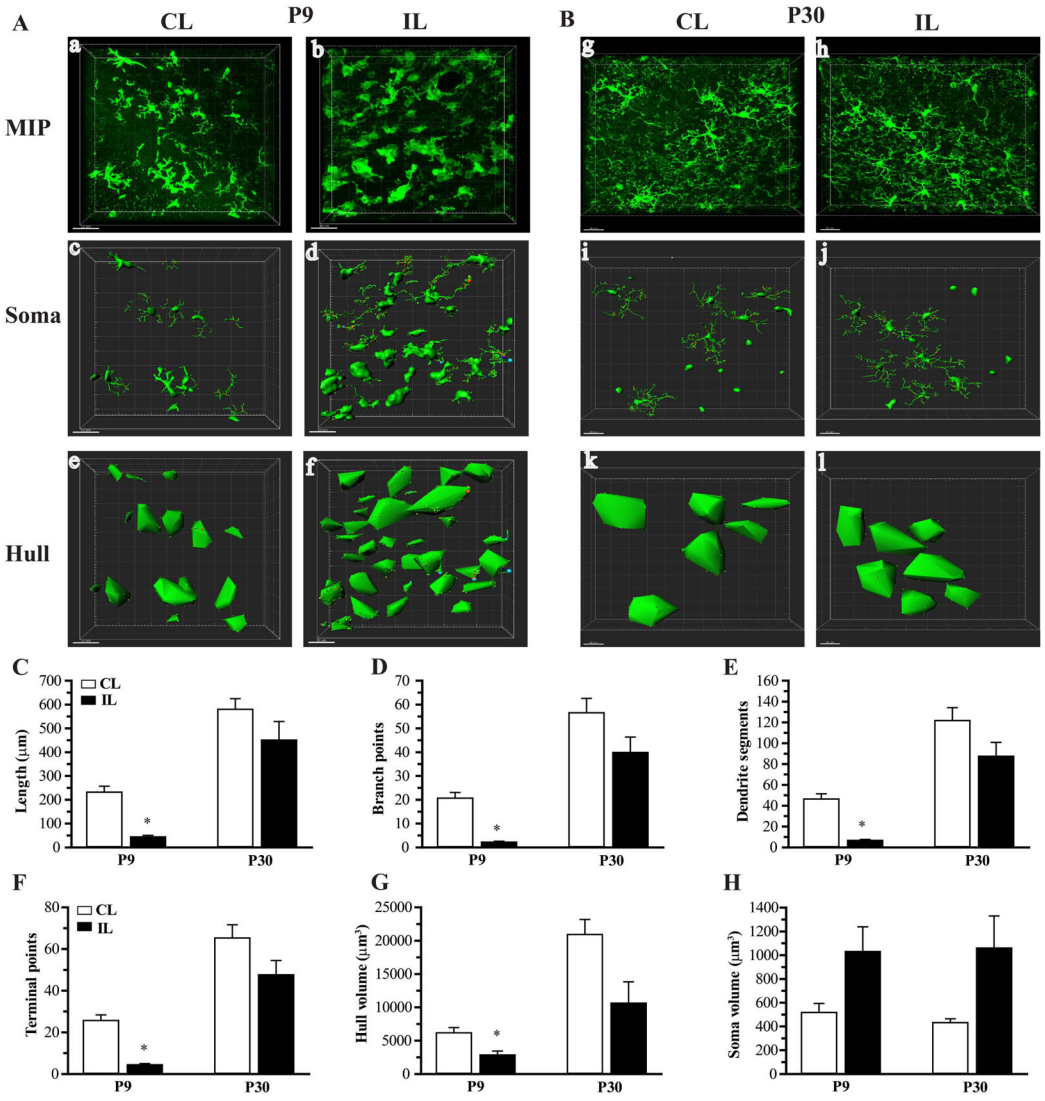

Figure 5: Quantification of changes in microglia morphology after hypoxia-ischemia.

Representative Imaris-processed images are shown in A and B from contralateral (CL) and ipsilateral (IL) hippocampus of P9 and P30 mice at 2 days post-HI. MIP images (a,b,g,h) demonstrate loss of branching in ipsilateral P9 microglia. Soma surface renders (c,d,i,j) illustrate an increase in soma size in ipsilateral brain regions, and Hull volumes (e,f,k,l) decrease in ipsilateral P9. Quantifications of cell process total length (C), number of branch points (D), segments (E) and terminal points (F), hull volume (G) and soma volume (H) are shown. N=5-10 microglia/region/mouse, 6 mice/group, Mean ± SEM. *p<0.05 vs CL.

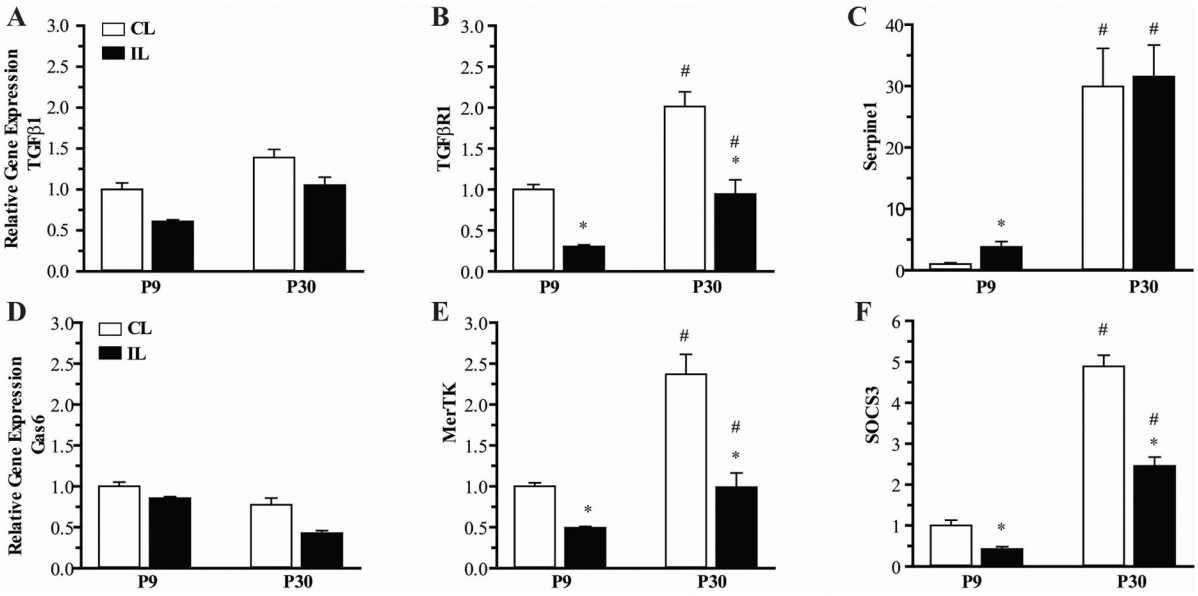

Figure 6: Age-dependent differences in activation of TGF-β and TAM Kinase pathways in CD11b+ microglia/macrophages after hypoxia-ischemia.

Expression of ligand (A, D), receptor (B, E) and downstream effector (C, F) in the TGF-β and MerTK signaling pathways at 2 days post-HI is shown for microglia isolated from ipsilateral and contralateral hippocampus of P9 and P30 mice. N=7-8 mice/group, Mean ± SEM. *p<0.05 vs contralateral CL hippocampus, #p<0.05 vs P9 brain region.